

Wavelet Transform for Visibility Analysis in Fog Situations

Christoph Busch¹, Eric Debes^{1,2}

¹ Computer Graphics Center, Rundeturmstr. 6, D-64283 Darmstadt, Germany,
email:busch@igd.fhg.de

² Supélec, Plateau de Moulon, 91192 Gif-sur-Yvette Cedex, France
email:debes@epfl.ch

Abstract

In this article a new technique for the estimation of the distance of visibility in fog conditions is presented. It is based on a psychovisual model and on contrast estimation with wavelet transform. For this application, specific B-spline wavelets are introduced in order to have a good space and frequency localization and to enable a fast implementation. Using images stemming from situations on motorways, this technique is compared to a direct local contrast calculation.

1. Introduction

Over the last few years, a growing number of Computer Vision system have been developed for traffic analysis and control on urban traffic and freeway roads. Increasing traffic on one hand and steady efforts for improved drivers security on the other hand abetted the development of sophisticated video-based systems that provide statistical measures of traffic flow for actual traffic information on variable message signs (VMS). Investigations have shown that variable message signs reduce traffic jams and thus minimize the burden on financial and environmental resources. Moreover it has been proven that traffic control systems also reduce the number of accidents down to 45% [3].

An information that can be particularly interesting for drivers is the visibility in fog situations. Fog is a real nuisance for motorists and causes a lot of accidents. The places where fog arises frequently are often well known. This leads to more and more message signs being installed in such places to inform motorists of the presence of fog. Such message signs indicate the distance of visibility which is traditionally estimated with transmissiometers. This paper shows that conventional fog-detection sensors can be replaced by integrated functionality provided by a Computer Vision system. The underlying idea is to analyze videoframes used in traffic control system and derive a visibility distance measure with extended signal analysis techniques. Therefore we present a new method based

on a B-spline wavelet transform to estimate visibility. The task can be formulated as identification of the image area where sharp variation points disappear due to the temporal fog situation. Thus increasing foginess will lead to a lower number of image lines that show sufficient variations, when the videoframe is analyzed in an upward vertical direction.

This paper is organized as follows. In Section 2 we provide the basic notion of psychovisual perception in fog and we explain the relation between contrast, gradient and wavelets. In Section 3 we design B-spline wavelets to calculate the contrast in 2D signals. (An Introduction to B-spline theory is given in Appendix B). In Section 4, we compare the wavelet based method to calculate the visibility in fog conditions to a direct method based on calculation of the contrast on little masks.

2. Wavelets based Contrast Estimation

2.1. Psychovisual Perception in Fog

Visual perception is a rather complex mechanism, because it is based on space, time and frequency analysis. Different characteristics of the signal received by the visual system are coded in the brain : intensity, color, shape (contrast and direction) and movement (direction and speed). To be seen, an object has to stand out enough from background. That's why the perception of shapes depends on the contrast between the object and the background.

The contrast is usually defined as follows:

$$C = \frac{|I_o - I_b|}{I_o + I_b} \quad (1.)$$

where I_o is the intensity of the object and I_b is the intensity of the background.

In 1948, Duntley formulated a law that indicates that, in fog conditions, contrast decreases exponentially with distance :

$$C = C_0 e^{-Kd} \quad (2.)$$

where C is the contrast received by the visual system, C_0 is the real contrast, d is the distance and K is a attenuation coefficient that characterizes the fog conditions.

Contrast also plays an important role in the perception of movement, speed and of direction. The experiments of Stone and Thomson [8] have shown that the visual system cannot estimate correctly the speed of an object with a low contrast. Psychologists have studied the problem of vision in fog and have noticed that fog causes many errors in the estimation of the shape, of the distance and of the speed of an object [1].

To conclude this brief overview of psychovisual perception in fog, we can say that contrast is the origin of all psychovisual effects. Furthermore the measure of contrast is inde-

pendent of daylight illumination of the scene. This conclusion is confirmed by the experiments of DeYoe and Van Essen about the visual system of primates [2], which have shown that the spatial distribution of light intensity in an image is the origin of all other properties.

2.2. Contrast, Gradient, Edges and Wavelets

In last section, we have noticed that contrast is the origin of visual perception. If one wants to determine what can be seen in fog, one needs to quantify the contrast and compare this value to a reference value that operates as a threshold. Experiments have shown that there is a high correlation between the contrast of different grey-level areas and the value of the gradient in the region where the contrast is measured. A low contrast corresponds to a low gradient and vice versa. This connection is due to the fact that contrast and gradient both characterize local variations in grey levels.

What can be seen in fog is in fact only high gradients in the different grey levels. When driving in fog, only the parts of the image characterized by high contrast (or high gradient) are utilized by the visual system. This is the reason why to determine if a pixel is visible, one just needs to calculate the gradient. If the gradient in this pixel is higher than a threshold corresponding to a 5% contrast, it indicates that this pixel is visible for the driver. The 5% contrast threshold has been defined by the CIE (International Commission on Lighting) and is the sufficient contrast for a human eye to see the difference between two gray-levels.

There is a close correlation of gradient measure and edge detection techniques. Since our approach is based on multiscale edge detection, we give in Appendix A a review of the Wavelet based edge detection's theory developed by Mallat and Hwang in [6] and we explain how this theory can be used to calculate the gradient in 2D signals.

However it can be shown that the gradient can be expressed through the wavelet transform and furthermore that the modulus M of the gradient is proportional to :

$$M f(x,y) = \sqrt{|W^1 f(x,y)|^2 + |W^2 f(x,y)|^2} \quad (3.)$$

In the edge detection theory developed by Mallat, the angle α of the gradient is also taken into account, so that the edge points are located in points where the modulus M has a local maximum in the direction α . However, our aim is to calculate the gradient and not to detect edges so for our application we do not need to calculate the angle. We simply calculate the gradient for each point of our image and if this gradient is higher than a value corresponding to a 5% contrast, then the pixel is visible regardless of the orientation of the corresponding edge.

3. B–Splines based Contrast Estimation

3.1. The Gaussian Kernel and B–Splines

The proper choice of the smoothing function $\theta(x, y)$ is the essential task to solve. For edge detection we need a function that is well localized in the frequency and in the spatial domain ; in particular, the variance Δx of the filter and the variance $\Delta \omega$ of the filter's spectrum should be small. It is well known that these two localization requirements are conflicting. Marr and Hildreth have used the Gaussian kernel for edge detection [7], because this function optimizes the Heisenberg uncertainty principle, which state that :

$$\Delta x \Delta \omega \geq \frac{1}{4} \pi \quad (4.)$$

Another reason why the gaussian kernel is often used in edge detection is that the response of human retina resembles a gaussian function. This has been confirmed by biological experiments. Neurophysiological research by Young [12] has shown that there are receptive field profiles in the mamalian retina and visual cortex, whose measured response profiles can be modeled well by superposition of Gaussian derivatives. Therefore, the Gaussian function is suitable for modeling the human visual system.

In practice, since computational load becomes extremely high with the Gaussian when the scales get large, many techniques have been proposed for efficient implementation of scale–space filtering in Computer Vision. Poggio et al. for example have used B–splines to approximate the gaussian kernel with an efficient implementation [9].

The advantages of B–splines in comparison with the Gaussian kernel lie in these functions leading to fast implementations and that they are still a good approximation to the Gaussian kernel. K. Torachi et al. review the merit of a window represented by B–splines in comparison with Gaussian and other well–established filters. In [11], Unser, Aldroubi and Eden have proven that both the B–splines and their Fourier transforms converge to the Gaussian function as the order of the spline tends to infinity :

$$\beta^n(x) \approx \sqrt{\frac{6}{\pi(n+1)}} \exp\left(-\frac{6x^2}{n+1}\right) \quad (5.)$$

In fact, by experiment it can be shown that the cubic B–spline is already nearly optimal in terms of time/frequency localization in the sense that its variance is within 2% of the limit specified by the uncertainty principle.

Both the physiological and biological experiments have shown that the human visual system can be modeled with a Gaussian kernel. Therefore, the B–spline is also suitable for modeling biological vision due to its similarity to Gaussian functions. But, since a fast implementation can be expected using the B–spline approach, it is preferable to select the

B-spline rather than the Gaussian function to calculate the contrast in an image with a good model.

3.2. The Choice of B-splines for Edge Detection

The theory of B-spline kernel is an area that has already been thoroughly investigated. In Appendix B we will give the definition and a brief review of the properties of these functions. A complete description of this theory can be found in [10].

If we use the B-splines as a smoothing function, we can define B-spline wavelets of order n as the first derivative of this function:

$$\psi^n(x) = \frac{d}{dx} \beta_{2^{-1}}^{n+1}(x) = 2(\beta^{n+1})^{(1)}(2x) \quad (6.)$$

which can be used for local extrema detection.

The Fourier Transform of these Wavelets is given by :

$$\hat{\psi}^n(\omega) = i\omega \hat{\beta}^{n+1}\left(\frac{\omega}{2}\right) = i\omega \left(\text{sinc}\frac{\omega}{4}\right) \left(\text{sinc}\frac{\omega}{4}\right)^{n+1} \quad (7.)$$

From the derivative property of the B-spline :

$$\frac{d}{dx} \beta^{n+1}(x) = \beta^n\left(x + \frac{1}{2}\right) - \beta^n\left(x - \frac{1}{2}\right) \quad (8.)$$

it is easy to infer that these two wavelets can also be written in the time domain as :

$$\psi^n(x) = 4 \left(\beta^n(2x + 1) - \beta^n(2x - 1) \right) \quad (9.)$$

These equations show that the wavelet functions can be considered as the first order difference of n th order B-splines at resolution level 2^{-1} , so they are good approximation of differentiation.

With the wavelet defined in (6.) we can detect edges for different scales. Thanks to the two scale relation (see 51. in Appendix B) and with dyadic scale $s = 2^j$, $j \in Z$, a fast algorithm can be designed to calculate the transform.

The Wavelet (6.) satisfies the two-scale relation :

$$\frac{1}{2} \psi^n\left(\frac{x}{2}\right) = \sum_k g_k \beta^n(x - k) \quad (10.)$$

or in the frequency domain :

$$\hat{\psi}^n(2\omega) = G(\omega) \hat{\beta}^n(\omega) \quad (11.)$$

where the frequency transfer function G is :

$$G(\omega) = \frac{\hat{\psi}^n(2\omega)}{\hat{\beta}^n(\omega)} = \sum_k g_k e^{-ik\omega} \quad (12.)$$

For the Wavelet (6.) $G(\omega)$ results in :

$$G(\omega) = 4i \sin\left(\frac{\omega}{2}\right) e^{i\frac{\omega}{2}} \quad (13.)$$

In this case, ψ^n is shifted by $1/2$ with a minor modification for FIR derivation. The FIR coefficients are :

$$\begin{cases} g_0 = -2 \\ g_1 = 2 \\ g_k = 0 \quad (k \neq 0, n \neq 1) \end{cases} \quad (14.)$$

The two scale relation (51.) allows one to use the following recursive algorithm:

$$\begin{cases} S_{2^j} f(n) = \sum_k h_k S_{2^{j-1}} f(n - 2^{j-1}k) \\ W_{2^j} f(n) = \sum_k g_k S_{2^{j-1}} f(n - 2^{j-1}k) \quad j = 1, 2, \dots, J \end{cases} \quad (15.)$$

where

$$W_{2^j} f = f * \psi_{2^j}^n \quad (16.)$$

is the wavelet transform and

$$S_{2^j} f = f * \beta_{2^j}^n \quad (17.)$$

is the smoothing operator.

The results for the one dimensional case can easily be extended to two dimensions. In this case, the smoothing function is defined as :

$$\beta^n(x, y) = \beta^n(x) \beta^n(y) \quad (18.)$$

and the 2D wavelet transform is given by :

$$W_{2^j} f(x, y) = \begin{bmatrix} W_{2^j}^1 f(x, y) \\ W_{2^j}^2 f(x, y) \end{bmatrix} = \begin{bmatrix} f * \psi_{2^j}^{n,1}(x, y) \\ f * \psi_{2^j}^{n,2}(x, y) \end{bmatrix} \quad (19.)$$

where

$$\psi^{n,1}(x, y) = \psi^n(x) \beta^n(y) , \quad \psi^{n,2}(x, y) = \psi^n(y) \beta^n(x) \quad (20.)$$

and $\psi^n(x)$ is the same wavelet as in the one dimensional case defined in relation (6.). With relation (19.),

$$W_{2^j} f(x, y) = 2^j \vec{\nabla} (f * \beta_{2^j}^n)(x, y) = 2^j \begin{bmatrix} \frac{\partial}{\partial x} (f * \beta_{2^j}^n)(x, y) \\ \frac{\partial}{\partial y} (f * \beta_{2^j}^n)(x, y) \end{bmatrix} \quad (21.)$$

one gets the partial derivation and thus the gradients according to the main axes.

The relation (52.) and (11.) can be extended to the two dimensional case :

$$\hat{\beta}^n(2\omega_x, 2\omega_y) = H(\omega_x)H(\omega_y)\hat{\beta}^n(\omega_x, \omega_y) \quad (22.)$$

$$\hat{\psi}^{n,1}(2\omega_x, 2\omega_y) = G(\omega_x)\hat{\beta}^n(\omega_x, \omega_y) \quad (23.)$$

$$\hat{\psi}^{n,2}(2\omega_x, 2\omega_y) = G(\omega_y)\hat{\beta}^n(\omega_x, \omega_y) \quad (24.)$$

Extending relation (17.) we formulate the smoothing operator :

$$S_{2^j} f(x, y) = f * \beta_{2^j}(x, y) , \beta_{2^j}(x, y) = \frac{1}{2^j} \beta\left(\frac{x}{2^j}, \frac{y}{2^j}\right) \quad (25.)$$

so that the fast recursive algorithm can be expressed as follows :

$$\begin{cases} S_{2^j} f = S_{2^{j-1}} f * (h, d)_{\uparrow 2^{j-1}} \\ W_{2^j}^1 f = S_{2^{j-1}} f * (d, g)_{\uparrow 2^{j-1}} \\ W_{2^j}^2 f = S_{2^{j-1}} f * (g, d)_{\uparrow 2^{j-1}} \end{cases} \quad (26.)$$

where $I * (h, g)_{\uparrow 2^{j-1}}$ is the convolution of the lines and columns of the image signal with the one–dimension filter $[h]_{\uparrow 2^{j-1}}$ and $[g]_{\uparrow 2^{j-1}}$ respectively. The sign d stands for the Dirac filter, whose impuls is equal to 1 for $n = 0$ and 0 otherwise.

With this method the two components of the wavelet transform are proportional to the two components of the gradient $\vec{\nabla}(f * \beta_{2^j}^n)$. For each scale 2^j the modulus of the gradient vector is proportional to :

$$M_{2^j} f(x, y) = \sqrt{|W_{2^j}^1|^2 + |W_{2^j}^2|^2} \quad (27.)$$

Each pixel for which the gradient is higher than a threshold value is visible through fog. In order to determine the threshold value corresponding to a contrast of 5%, the wavelet transform is calculated on an test image with a contrast of 5%. The threshold is taken as the highest value of the resulting transform. This will be found at the position of the edge between the two different greylevel areas.

4. Comparison of the Wavelet based Method to a direct Calculation of the Contrast

The goal of this paper is to determine the distance of visibility in fog conditions from images taken by a video camera that is installed overhead a traffic lane motorway. To determine the contrast, we have used two methods :

- the first one is based on the direct calculation of the contrast
- the second one is based on the theory of edge detection

In this section, we present the results for the two methods with two images taken with a video camera :

- the first image was taken in a clear atmosphere and with good visibility
- The second image was taken in fog conditions with a distance of visibility of about 100m.



Fig 1 : An image in clear atmosphere (left) and in fog conditions (right)

4.1. Direct Contrast Calculation

In this section, we present the first method, that aims at determining the distance of visibility directly, on the raw data provided by the video sensor. The quantification of the contrast is calculated directly on a mask of a few pixels.

The crucial problem lies in the choice of the mask's size. In our application, areas of sharp variations points and high contrast are located along white traffic lane marking and the border of the road. These areas are essential for drivers perception of the road in fog situations. Due to the fact that raw data provided by the camera is used for other traffic control tasks at the same time (traffic count and velocity measures) the view of the camera covers

the entire road. Thus sharp variations take place in a two or three pixel neighborhood. Therefore the size of the mask has been chosen to be very small (3x3 pixels).

The image is analyzed from the bottom to the top and for each pixel the contrast is derived using the definition of the contrast (1.). Since we look for the highest contrast, we take the intensity of the object equal to I_{\max} and the intensity of the background equal to I_{\min} so that the contrast is given by :

$$C = \frac{I_{\max} - I_{\min}}{I_{\max} + I_{\min}} \quad (28.)$$

The last pixel for which the contrast is higher than 5% is considered as last visible pixel. The coordinates of the pixel are then used to estimate the distance of visibility with a transformation from the image coordinates to the world coordinates, according to the precalculated outer orientation. The parameters for this transformation are given with the outer orientation, that describes the plane (image plane) to plane (traffic plane) relation. This task initially needs to be done during system calibration.

We have defined a region of interest, which defines the part of the image where the contrast has to be calculated. This region has been introduced to exclude those pixels from consideration that do not correspond to the traffic lane itself used for calibration. For example, one can see on Fig. 1 the roadlights that correspond to a line that is high in the image so that they would correspond to a large distance with the transformation from image coordinates to world coordinates. To remedy this impact, those pixels should not be considered for contrast estimation; this is the reason for introducing a region of interest to define the interesting part of the image for contrast estimation.



Fig 2 : The region of interest

4.2. Wavelet Transform for Contrast Estimation

This method has already been explained in Section 3. To choose the Wavelet function we had to make a choice between a good localization, which requires a small window and good noise removal that needs a large window. We show the results for three types of wa-

velets with different support lengths : first the splines from Michael Unser with an FIR filter with 27 coefficients, then the splines given by Mallat in one of his papers on multi-scale edges [5] and at the end the splines that have been calculated in section 3.

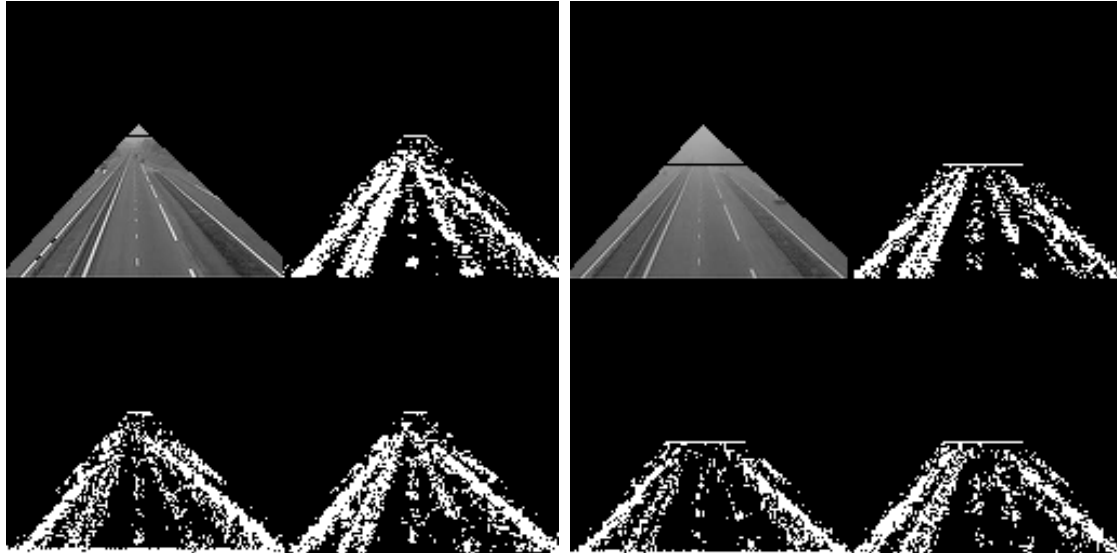


Fig 3 : Results with B-spline wavelets proposed by Unser for the image with a clear atmosphere (left) and for the image in fog conditions (right)

Figures 3 shows the Wavelet Transform in the first iteration. It's obvious that these wavelets are too large for our application. This comes from the fact that B-spline wavelet functions are convoluted with the image, they take into account the variation that are located in neighboring pixels in the measure of the contrast. For our application we need wavelet functions with a smaller support. It's the case for the wavelet function of Mallat :

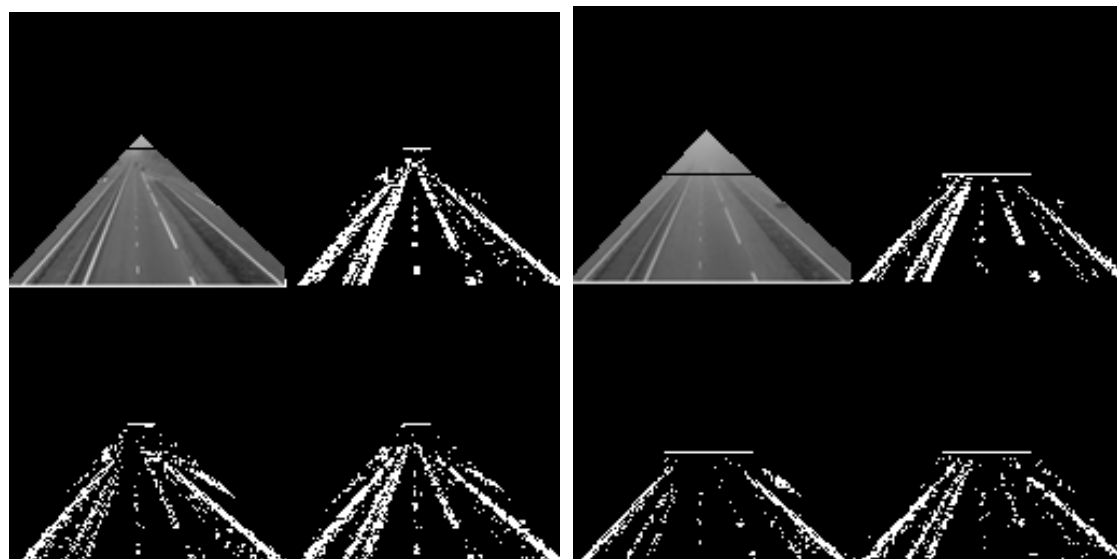


Fig 4 : Results with Mallat spline for the image with a clear atmosphere (left) and for the image in fog conditions (right)

The wavelet that we have calculated in Section 3 have the advantage to introduce almost no blurring in the resulting images, because only the pixels where the variation occur are taken into account in the calculation of the contrast. These wavelets fit very good to our application, because we just want to detect variations that happen between two or three neighboring pixels. We show the resulting images for this type of wavelets :

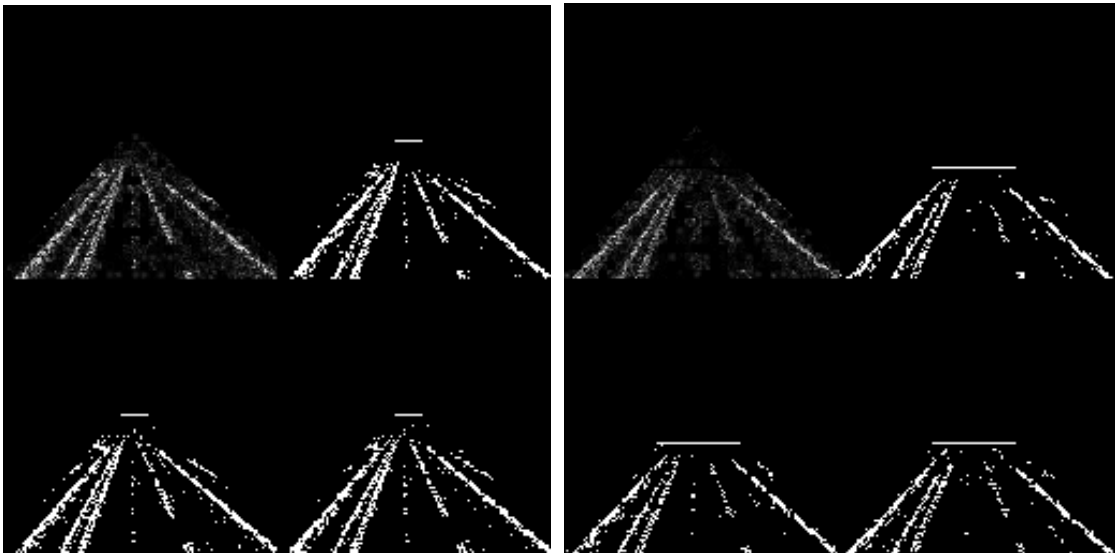


Fig 5 : Results with the splines of section 3.2. for the image with a clear atmosphere (left) and for the image in fog conditions (right)

The distance of visibility is calculated with a transformation from image coordinates to world coordinates. If the distance of visibility is higher than 1000 m (like in the first image), according to the definition of fog given by the German federal traffic department, there is no fog. A visibility between 1000m and 300m is given with a rounding to the nearest multiple of 50m and a distance of visibility smaller than 300m is given with a rounding to the nearest multiple of 10m. For example, the distance of visibility is 120m for the right image. The accuracy of our system is much better than what we need to give such results, because the precision depends of the distance in real world between two image pixels. For a distance between 1000m and 300m, this distance is much smaller than 50m and for a distance between 300m and 50m, it is much smaller than 10m. According to these requirements and specifications our system gives very good results for this application.

5. Conclusion

We have noted that visual perception in fog is based on the perception of contrast. Due to its psychophysiological foundation, Mallat's theory for edge detection is well suited to estimate gradients in an image and hence to describe the visibility in fog situations. In order to overcome the drawbacks that arise with the limited resolution of video frames, we have presented B-splines with specific small support that are capable of fog detection.

The application of the B-spline approach gives good results for the detection of the distance of visibility in direct comparison to a contrast-based method. Even though the accuracy of the two compared methods only differs slightly, the wavelet-based approach has a major advantage in its close similarity to the perceptual system of the driver since it bases on Mallat's vision model. This theory is much closer to the human visual system than the contrast theory. Indeed, it takes into account not only the direct difference of intensities between objects but also the gradient of the intensity in the scene, which is exactly what happens in the human visual system.

The primary application of the techniques presented in this paper was the analysis of video frames taken from overhead a traffic lane. With this methodology it's possible to inform drivers in real time of the presence of fog through variable message sign located a few kilometers before the foggy area. It is evident that the wavelet based approach, which analyzes the entire traffic scene globally, will provide a more precise input to fog information systems than the traditional transmissiometers that analyze the fog density locally aside the roadway. Thank to improved information through variable message signs, it will be possible to avoid accidents with very often tragic issue. Another possible application is an individual driving support system that improves the drivers vision of the traffic scene. In this case, one could display an image that shows a much brighter and sharper view of the road directly on the windshield of the car or on a separate monitor integrated in the dashboard. This can be reached with a combination of the wavelet-based edge detection that elaborates all significant edges of an image influenced by fog and an additional contrast enhancement based on the method of Lu [4] including an inverse transform of the modified coefficients.

Appendix A

Multiscale Edge Detection

Most edge detectors smooth the signal at different scales and detect sharp variations with the first or second derivative of the signal. The extrema of the first derivative correspond to the zero-crossings of the second derivatives and to the inflexion points of the smoothed signal. The smoothing function is defined as a function $\theta(x)$ for which :

$$\int_{-\infty}^{+\infty} \theta(x)dx = 1 \quad (29.)$$

$$\lim_{x \rightarrow \pm\infty} \theta(x) = 0 \quad (30.)$$

The function $\theta(x)$ is often chosen as a Gaussian. We require that $\theta(x)$ is differentiable and we define a wavelet as the first derivative of this function :

$$\psi^a(x) = \frac{d}{dx} \theta(x) \quad (31.)$$

$\psi^a(x)$ can then be considered as a wavelet because its integral is equal to zero.

$$\int_{-\infty}^{+\infty} \psi^a(x) dx = 0 \quad (32.)$$

Let $f(x)$ be a real function in $L^2(\mathbb{R})$. In order to detect edges of $f(x)$ at different scales s , we define the dilatation of the function $\theta(x)$ by a factor m :

$$\theta_m(x) = \frac{1}{m} \theta\left(\frac{x}{m}\right) \quad (33.)$$

With this definition, edges at the scale m can be detected at local sharp variation points of $f(x)$ smoothed by $\theta_m(x)$.

The wavelet transform of $f(x)$ for the wavelet function given in (31.) is defined as :

$$W_m^a f(x) = f * \psi_m^a(x) \quad (34.)$$

The wavelet transform can also be expressed as follows :

$$W_m^a f(x) = f * m \frac{d\theta_m}{dx}(x) = m \frac{d}{dx} (f * \theta_m)(x) \quad (35.)$$

As Mallat shows in [6], the wavelet transform W_m^a is proportional to the first derivative of $f(x)$ smoothed by $\theta_m(x)$. If $\theta(x)$ is chosen as a Gaussian, then the detection of local extrema of W_m^a is equivalent to the Canny edge detector. When the scale m is large, the small discontinuities are eliminated through convolution of the function f with $\theta_m(x)$; this is why only sharp variations are detected if m is large.

The Canny edge detector is easily extended to the two dimensional case. For this purpose, we define a smoothing function of two variables $\theta(x, y)$ with the following properties :

$$\int_{-\infty}^{+\infty} \int_{-\infty}^{+\infty} \theta(x, y) dx dy = 1 \quad (36.)$$

$$\lim \theta(x, y) = 0 \quad (37.)$$

and the dilatation by a scale factor m of this function :

$$\theta_m(x, y) = \frac{1}{m^2} \theta\left(\frac{x}{m}, \frac{y}{m}\right) \quad (38.)$$

The image is smoothed for different scales through convolution with $\theta_m(x, y)$. Then, like in the one-dimensional case, the gradient vector can be calculated with the wavelet transform. The edge points are the points where the modulus of the gradient vector is maximal. To calculate the gradient, we define two wavelet functions $\psi^1(x)$ and $\psi^2(x)$:

$$\psi^1(x, y) = \frac{\partial \theta(x, y)}{\partial x} \quad (39.)$$

and

$$\psi^2(x, y) = \frac{\partial \theta(x, y)}{\partial y} \quad (40.)$$

The corresponding wavelet transforms are :

$$W_m^1 f(x, y) = f * \psi_m^1(x, y) \quad (41.)$$

and

$$W_m^2 f(x, y) = f * \psi_m^2(x, y) \quad (42.)$$

To facilitate a fast implementation, the scales are chosen as dyadic, i.e. $m = 2^j$, $j \in \mathbb{Z}$ so that the gradient can be expressed as :

$$\begin{bmatrix} W_{2^j}^1 f(x, y) \\ W_{2^j}^2 f(x, y) \end{bmatrix} = 2^j \begin{bmatrix} \frac{\partial}{\partial x} (f * \theta_{2^j})(x, y) \\ \frac{\partial}{\partial y} (f * \theta_{2^j})(x, y) \end{bmatrix} = 2^j \nabla (f * \theta_{2^j})(x, y) \quad (43.)$$

For every scale 2^j , the modulus M of the gradient is proportional to :

$$M_{2^j} f(x, y) = \sqrt{|W_{2^j}^1 f(x, y)|^2 + |W_{2^j}^2 f(x, y)|^2} \quad (44.)$$

Appendix B

The Theory of B-splines

The central continuous B-spline of order n is denoted $\beta^n(x)$ and can be generated by repeated n convolutions of a B-spline of order 0 :

$$\beta^n(x) = \beta^0 * \beta^{n-1} \quad (45.)$$

where the 0th order B-spline $\beta^0(x)$ is the window function with support $\left[-\frac{1}{2}, \frac{1}{2}\right]$.

The spectrum of this function is given by :

$$\hat{\beta}^n(\omega) = \left[\hat{\beta}^0(\omega) \right]^{n+1} = \left[\frac{\sin\left(\frac{\omega}{2}\right)}{\frac{\omega}{2}} \right]^{n+1} = \text{sinc}^{n+1}\left(\frac{\omega}{2}\right) \quad (46.)$$

For an integer $m \geq 1$, $\beta_m^n(x)$ is the n th order B-spline dilated by a scale factor m :

$$\beta_m^n(x) = \frac{1}{m} \beta^n\left(\frac{x}{m}\right) \quad (47.)$$

Consider now a sequence of embedded polynomial spline function $S_{(i)}^n$, $i \in \mathbb{Z}$ (n , an odd integer is the degree of the polynomial). For every $i \in \mathbb{Z}$, $S_{(i)}^n$ is a subspace of L^2 and belongs to class C^{n-1} . On each interval $[k2^i, (k+1)2^i]$ ($k \in \mathbb{Z}$), $S_{(i)}^n$ are equivalent to a polynomial of order n :

$$S_{(i)}^n = \left\{ g_{(i)}^n(x) = \sum_{-\infty}^{+\infty} c_i(k) \beta_{2^i}^n(x-2^i k), (x \in \mathbb{R}, c_i \in l_2) \right\} \quad (48.)$$

$S_{(i)}^n$, $i \in \mathbb{Z}$ constitutes a multiscale or multiresolution approximation of L^2 , i.e. :

$$S_{(i+1)}^n \subset S_{(i)}^n, i \in \mathbb{Z} \quad (49.)$$

and

$$\lim_{i \rightarrow \infty} S_{(i)}^n = L^2 \quad (50.)$$

Any Signal $f \in L^2$ can be represented as a weighted sum of translated and dilated B-splines and are completely determined by the coefficients $c_i(k)$.

The nesting relation (49.) for $i=1$ can be written $S_1^n \subset S_0^n$. Since $\beta^n\left(\frac{x}{2}\right) \in S_0^n$, we have the following two-scale relation :

$$\frac{1}{2} \beta^n\left(\frac{x}{2}\right) = \sum_{k=-\infty}^{+\infty} h_k \beta^n(x-k) \quad (51.)$$

or its equivalent in the Fourier domain :

$$\hat{\beta}^n(2\omega) = H(e^{i\omega}) \hat{\beta}^n(\omega) \quad (52.)$$

where

$$H(e^{i\omega}) = \sum_k h_k e^{ik\omega} = \frac{\hat{\beta}^n(2\omega)}{\hat{\beta}^n(\omega)} = \frac{\text{sinc}^{n+1}\frac{\omega}{2}}{\text{sinc}^{n+1}\frac{\omega}{2}} = \left(\cos\frac{\omega}{2}\right)^{n+1} = \left(\frac{e^{i\frac{\omega}{2}} + e^{-i\frac{\omega}{2}}}{2}\right)^{n+1} \quad (53.)$$

$$H(e^{i\omega}) = \sum_{j=0}^{n+1} \frac{1}{2^{n+1}} \binom{n+1}{j} e^{i[j - \frac{(n+1)}{2}]\omega} \quad (54.)$$

The FIR filter coefficients are the coefficients of $H(e^{i\omega})$ in the base $(e^{ik\omega})$, so that if equation (54.) is projected on $e^{ik\omega}$, we get directly the FIR coefficients h_k for n odd :

$$h_k = \begin{cases} \frac{1}{2^{n+1}} \binom{\frac{n+1}{2} + k}{k} , & \text{if } |k| \leq n+1 \\ 0 , & \text{otherwise} \end{cases} \quad (55.)$$

For n even, if the central B-spline $\beta^n(x)$ is shifted by half a sampling step with respect to the origin ; it is then called a causal B-spline. For simplicity we still denote this function by $\beta^n(x)$ with the abuse of notation. In this case, we have:

$$H(e^{i\omega}) = \sum_k h_k e^{ik\omega} = e^{i\frac{\omega}{2}} \left(\cos \frac{\omega}{2} \right)^{n+1} = e^{i\frac{\omega}{2}} \left(\frac{e^{i\frac{\omega}{2}} + e^{-i\frac{\omega}{2}}}{2} \right)^{n+1} \quad (56.)$$

$$H(e^{i\omega}) = \sum_{j=0}^{n+1} \frac{1}{2^{n+1}} \binom{n+1}{j} e^{i[j-\frac{n}{2}]\omega} \quad (57.)$$

In this case, the FIR filter coefficients can also be obtained through projection of equation (57.) on the vectors of the base ($e^{ik\omega}$), so that for n even the corresponding FIR filter coefficients are :

$$h_k = \begin{cases} \frac{1}{2^{n+1}} \binom{\frac{n}{2} + k}{k} , & \text{if } -\frac{n}{2} \leq k \leq \frac{n}{2} + 1 \\ 0 , & \text{otherwise} \end{cases} \quad (58.)$$

The two-scale relation (51.) makes B-spline very attractive for wavelet theory and multi-scale analysis. These properties can be extended to the discrete space so that the discrete sampled B-spline can define a family of multiresolution approximation spaces of l^2 :

$$s_i^n = \left\{ v \in l^2, v(j) = \sum_{k \in \mathbb{Z}} c_i(k) b_i^n(j - 2^i k) , c_k \in l^2 \right\} \quad (59.)$$

where $b_i^n(j) = \beta^n\left(\frac{j}{2^i}\right)$ represents the discrete sampled spline with n odd and $j \in \mathbb{Z}$.

l^2 consists of all summable discrete sequences with finite energy. The embedding or refinement relations between the discrete spaces s_i^n still holds the same properties for the continuous polynomial spline of order n :

$$\lim s_i^n = l^2 , s_{i+1}^n \subset s_i^n , (\forall i \in \mathbb{Z}) \quad (60.)$$

References

- [1] Brown I.D. Driving in Fog, Report of a Symposium "Eyes on the Road", England, pp. 26-27, November 1983

- [2] DeYoe E.A., VanEssen D.D. Concurrent Processing Streams in Monkey Visual Cortex, *Trends in Neuro Sciences*, vol. 11, no. 5, pp. 219–226, 1988
- [3] Hogema, J.H. et al. : Evaluation of an automatic fog–warning system, *Traffic Engineering and Control*, pp. 629–632, 1996
- [4] Lu J., Healy D.M.Jr., Weaver: Contrast Enhancement via Multiscale Gradient Transformation, *Proceedings of the International Conference on Image Processing*, September 1996.
- [5] Mallat S., Zhong S. Characterization of Signals from Multiscale Edges, *IEEE Transactions on Pattern Analysis and Machine Intelligence*, vol. 14, No. 7, July 1992
- [6] Mallat S., Hwang W.L. Singularity Detection and Processing with Wavelets, *IEEE Transactions on Information Theory*, vol. 38, no. 2, march 1992
- [7] Marr D., Hildreth E., Theory of edge detection, *Proc. Roy. Soc. London*, vol. B207, pp. 187–217, 1980.
- [8] Stone L.S., Thomson P. Effect of Contrast on Human Speed Perception. NASA Technical Memorandum 103898, December 1992
- [9] Torre V., Poggio T.A. On Edge Detection, *IEEE Trans. PAMI*, vol. 8, pp. 147–163, 1986
- [10] Unser M., Aldroubi A., Eden M. : B–Spline Signal Processing : Part I and II, *IEEE Transactions on Signal Processing*, vol. 41, no. 2, Feb. 1993
- [11] Unser M., Aldroubi A., Eden M. : On asymptotic Convergence of B–Spline Wavelets to Gabor Functions, *IEEE Transactions on Information Theory*, vol. 38, no. 2, March 1992
- [12] Young R. A. The Gaussian Derivative Model for Machine Vision : Visual Cortex Simulation, *J. Opt. Amer. Soc.*, July 1987.